Biomedicine & Pharmacotherapy 178 (2024) 117236

Contents lists available at ScienceDirect

Biomedicine & Pharmacotherapy

journal homepage: www.elsevier.com/locate/biopha

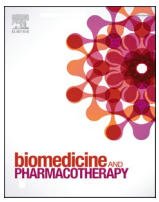

Long-term effects of luteolin in a mouse model of nephropathic cystinosis

Ester De Leo [a,*], Anna Taranta [a], Roberto Raso [a], Marco Pezzullo [b], Michela Piccione [c], Valentina Matteo [d], Alessia Vitale [e], Francesco Bellomo [a], Bianca Maria Goffredo [e], Francesca Diomedi Camassei [f], Giusi Prencipe [d], Laura Rita Rega [a], Francesco Emma [g]

[a] Laboratory of Nephrology, Bambino Gesù Children's Hospital, IRCCS, Rome, Italy
[b] Core Facilities, Bambino Gesù Children's Hospital, IRCCS, Rome, Italy
[c] Confocal Microscopy Core Facility, Research Laboratories, Bambino Gesù Children's Hospital, IRCCS, Rome, Italy
[d] Laboratory of Immuno-Rheumatology, Bambino Gesù Children's Hospital, IRCCS, Rome, Italy
[e] Laboratory of Metabolic Diseases, Bambino Gesù Children's Hospital, IRCCS, Rome, Italy
[f] Pathology Unit, Bambino Gesù Children's Hospital, IRCCS, Rome, Italy
[g] Division of Nephrology, Bambino Gesù Children's Hospital, IRCCS, Rome, Italy

ARTICLE INFO

Keywords:
Cystinosis
Fanconi syndrome
Luteolin
Apoptosis
Lysosome
Autophagy

ABSTRACT

In infantile nephropathic cystinosis, variants of the *CTNS* gene cause accumulation of cystine in lysosomes, causing progressive damage to most organs. Patients usually present before 1 year of age with signs of renal Fanconi syndrome. Cysteamine therapy allows cystine clearance from lysosomes and delays kidney damage but does not prevent progression to end-stage kidney disease, suggesting that pathways unrelated to cystine accumulation are also involved. Among these, impaired autophagy, altered endolysosomal trafficking, and increased apoptosis have emerged in recent years as potential targets for new therapies. We previously showed that luteolin, a flavonoid compound, improves these abnormal pathways in cystinotic cells and in zebrafish models of the disease. Herein, we have investigated if prolonged luteolin treatment ameliorates kidney damage in a murine model of cystinosis. To this end, we have treated *Ctns*$^{-/-}$ mice from 2 to 8 months with 150 mg/kg/day of luteolin. No significant side effects were observed. Compared to untreated animals, analyses of kidney cortex samples obtained after sacrifice showed that luteolin decreased p62/SQSTM1 levels ($p < 0.001$), improved the number, size, and distribution of LAMP1-positive structures ($p < 0.02$), and decreased tissue expression of cleaved caspase 3 ($p < 0.001$). However, we did not observe improvements in renal Fanconi syndrome and kidney inflammation. Kidney function remained normal during the time of the study. These results indicate that luteolin has positive effects on the apoptosis and endo-lysosomal defects of cystinotic proximal tubular cells. However, these beneficial effects did not translate into improvement of renal Fanconi syndrome.

1. Introduction

Cystinosis is a rare inherited lysosomal storage disease caused by mutations in the *CTNS* gene that encodes cystinosin, a lysosomal cystine/proton symporter [1]. Impairment of lysosomal cystine efflux leads to progressive accumulation and crystallization of cystine in virtually all organs. Infantile nephropathic cystinosis (OMIM 219800) is the most frequent and severe form of the disease, which is characterized by early-onset proximal tubular dysfunction, causing renal Fanconi syndrome [2]. Patients usually develop around 6 months of age failure to thrive, signs of dehydration, and rickets, that are secondary to abnormal urinary losses of water, salt, amino acids, phosphate, bicarbonate, glucose, and low-molecular-weight (LMW) proteins [3]. With time, the glomerular function also deteriorates. If untreated, most patients develop end-stage kidney disease around the age of 10 years [3,4]. Cysteamine has been introduced for the treatment of cystinosis in the 80's and is currently the only available treatment for the disease [5,6]. It allows clearance of cystine from lysosome but does not correct the

Abbreviations: ALT, alanine aminotransferase; AST, aspartate aminotransferase; CC16, clara cell 16 protein; CMA, chaperon-mediated autophagy; γGT, gamma-glutamyl transferase; H&E, hematoxylin and eosin; LAMP1, lysosomal associated membrane protein 1; LMW, low-molecular-weight; NLRP2, Nod-like receptor protein 2; P.A.S, periodic acid Schiff; PTCs, proximal tubular cells.

* Corresponding author.
E-mail address: ester.deleo@opbg.net (E. De Leo).

https://doi.org/10.1016/j.biopha.2024.117236
Received 4 June 2024; Received in revised form 24 July 2024; Accepted 30 July 2024

Fanconi syndrome when started after tubular dysfunction has developed and can only delay progression to end-stage kidney disease by 5–10 years if started early [3,4,7]. Although cysteamine has dramatically improved the life expectancy of patients [8], new therapies are needed. A clinical trial exploring the benefits of hematopoietic stem cell transplantation after *in vitro* gene therapy is currently ongoing [9]. In addition, studies carried during the past two decades in several laboratories have highlighted the complexity of cell changes caused by the invalidation of the *CTNS* gene. These involve several pathways, including enhanced apoptosis [10–13], mitochondrial dysfunction [14,15], oxidative stress [16–18], inflammation [19], aberrant macro- and chaperon-mediated autophagy (CMA) [20,21], endo-lysosomal dysfunction [22,23] and decreased expression of megalin and cubilin [22,24,25]. Some of these pathways are poorly responsive to cysteamine and represent novel potential targets for therapy that may complement cysteamine treatment [26,27].

Drug repurposing is a potentially useful strategy to identify new treatments for rare diseases [28,29]. We have recently focused on autophagy defects as a target to identify new treatments. Using an unsupervised cell-based drug screening strategy that included 1200 compounds (Prestwick Chemical Library, (Illkirch-Graffenstaden, France), most of which are approved for clinical use in humans, we have identified molecules that reduced the accumulation of the autophagy substrate p62/SQSTM1 in immortalized cystinotic human proximal tubular cells (PTCs) [30]. Among positive hits, we have further investigated the effects of luteolin (3',4',5,7-tetrahydroxyflavone), a natural flavonoid found in fruits and vegetables [31], using cell-based *in-vitro* assays and a zebrafish model of cystinosis [30]. Our results have shown that luteolin improves degradation of autophagy cargoes, restores normal intracellular lysosomal distribution, reduces the apoptosis rate, and stimulates endocytic processes [30]. Based on these promising results, we have performed a pre-clinical study to test the efficacy of luteolin in preventing kidney damage in cystinotic mice.

2. Materials and methods

2.1. Animal care and luteolin administration

Ctns$^{-/-}$ mice (C57BL/6 background) were kindly provided by Prof. Corinne Antignac [32]. Animal care and experimental procedures were conducted in accordance with the European 2010/63/EU directive on the protection of animals used for scientific purposes and were authorized by the Italian Ministry of Health (authorization number 1088/2020-PR). Wild type and *Ctns*$^{-/-}$ female mice (n = 6 per group) were fed from 2 to 8 months of age with a standard diet prepared in pellets (4RF21 diet, Mucedola Srl, Settimo Milanese, Italy) or with the same diet containing 1.1 g of luteolin per kg (Santa Cruz Biotechnology, Inc. Dallas, Texas, USA). The estimated corresponding doses of luteolin, based on daily food intake, was 150 mg/kg/day (average mouse weight: 22 g; average food intake: 3 g /day). This dose was tested in preliminary studies performed on a limited number of animals that were treated for up to 8 months, in which we observed no apparent toxic effects and good palatability (4 wild type and 4 *Ctns*$^{-/-}$ mice; 2 males and 2 females per group; data not shown).

Urine sampling was performed after mice were acclimatized in metabolic cages for 24 h. Urines were collected for 24 h in the presence of 0.1 % sodium azide and protease inhibitors (Thermo Fisher scientific, MA, USA). Mouse weight and length were recorded before entering metabolic cages. Urine samples were collected every two months, blood samples at sacrifice. Routine urine and serum analyses were performed in a veterinary laboratory (Appialab Srl, Rome, Italy). LMW proteinuria was estimated by measuring urinary Clara cell 16 protein (CC16) excretion (Biomatik Corporation, Ontario, Canada). Creatinine clearance was calculated with the following formula: creatinine clearance (ml/min) = urine creatinine (mg/dl) x 24 h-urine volume (ml) / serum creatinine (mg/dl) x 1440 min; data were normalized for body weight.

2.2. Histology, immunofluorescence, and immunohistochemistry

Liver and kidney specimens were formalin-fixed and embedded in paraffin. 2.5 μm-thick sections were obtained, dewaxed, and rehydrated. Sections were stained with hematoxylin/eosin (H&E) or Periodic Acid Schiff Kit (P.A.S.) (#04–130802, Bio-Optica, Milano, Italy). For immunohistochemistry and immunofluorescence, heat-induced epitope retrieval was performed by boiling slides in the presence of EDTA at pH 9 (Dako, Glostrup, Denmark) after dewaxing and rehydrating. Tissue slides were blocked in 5 % BSA and 2 % NGS for 1 h. Sections were incubated overnight at 4°C with the following primary antibodies: mouse monoclonal anti-p62/SQSTM1 antibody (1:300) (# H00008878-M01, Abnova, Taipei City, Taiwan), mouse monoclonal anti-LAMP1 antibody (1:100) (#sc-20011, Santa Cruz Biotechnology, Inc. Dallas, Texas, USA), rabbit polyclonal anti–active caspase-3 antibody (1:400) (9661; Cell Signaling Technology, Danve, MA, USA), rabbit polyclonal anti-CD68 antibody (1:100) (#PA5–78996, Thermo Fisher scientific, MA, USA). For immunofluorescence studies, primary antibodies were revealed with secondary Alexa Fluor antibodies (Applied Biosystems, Life Technologies, Carlsbad, CA, USA); nuclei were stained with 49,6-diamidino-2-phenylindole. For immunohistochemistry studies, primary antibodies were revealed with biotinylated secondary antibodies (K8024, Dako, Carpinteria, CA, USA) and the peroxidase DAB kit (Dako, Carpinteria, CA, USA). Counterstaining was performed with the Gill2 hematoxylin solution (Dako, Carpinteria, USA).

Microscopic images were acquired using the NanoZoomer S60 (Hamamatsu, Shizuoka, Japan) digital slide scanner platform equipped with an Olympus 20x/0.75 PlanSAPO objective. Fluorescence acquisition was performed with a linear ORCA-Flash 4.0 digital CMOS camera (Hamamatsu) mounted on a fluorescence imaging module equipped with a L11600 mercury lamp (Hamamatsu).

Confocal microscopy imaging was performed using an Olympus FV3000 laser-scanning confocal microscope (Evident Scientific, Hamburg, Germany) equipped with 405 nm and 488 nm laser sources. Sequential confocal images were acquired with UPLXAPO 60X or 40X oil immersion objectives (1.42 and 1.40 numerical aperture, respectively), using 1024 × 1024 image format and a scan speed of 8 μs/pixel. Laser's power, beam splitters, filter settings, pinhole diameter, and scan mode were the same for all samples.

To quantify staining (mean fluorescence intensity, number, and size of structure), at least 15 random fields for each experimental condition were analyzed blindly using the Image J software (https://imagej.net/).

To quantify histological lesions, a "tissue damage score" was created that included tubular atrophy, interstitial fibrosis, cortical tubular casts, glomerulosclerosis, and vascular damage. Each parameter was scored blindly by a pathologist (FDC) using a scale from 0 to 3 (0 = normal, 1 = mild lesions, 2 = moderate lesions, 3 = severe lesions). Results were added to generate a score ranging 0–15.

2.3. LC-MS-based cystine measurements

Tissues were homogenized in 10 mM N-ethylmaleimide (Merck, Darmstadt, Germany). Protein fractions were obtained after precipitation in 10 % 5-sulfosalicylic acid (Merck, Darmstadt, Germany) and centrifugation at 20,000 g for 20 min at 4°C. Protein pellets were resuspended in 100 mM NaOH (Merck, Darmstadt, Germany) and assayed by the Bio-Rad Protein Assay (Bio-Rad, CA, USA), according to the manufacturer's instructions. Supernatants (50 μL) were mixed with 50 μL of internal standard solution (Cystine d6) and vortexed for 5 s. The mixture was then extracted with 200 μL of acetonitrile, vortexed for at least 30 s, and centrifuged at 13,000 rpm for 9 min. Liquid chromatography and mass spectrometry analysis was performed by a UHPLC Agilent 1290 Infinity II 6470 (Agilent Technologies) equipped with an ESI-JET-STREAM source operating in the positive ion (ESI+) mode. The MassHunter Workstation (Agilent Technologies, CA, USA) software was used to control the equipment and to analyze data. The system was

equipped with a InfinityLab Poroshell 120 HILIC 1.9 μm 100 x 2.1 mm separation column (Agilent Technologies, CA, USA). Validation of the method was performed in agreement with the US Food and Drug Administration (FDA) guideline for industry bioanalytical method validation (FDA 2013) and the European Medicines Agency (EMA) guidelines (EMA 2011).

2.4. RNA extraction, quantitative real-time PCR

Total kidney RNA was extracted using the Animal Tissue RNA Purification Kit, (#25700, Norgen Biotek, Thorold, ON, Canada) and cDNA was synthesized using the Wonder RT-cDNA Synthesis Kit (#EME037050 EuroClone, Milano, Italy) according to the manufacturer's instructions. Real-time PCR assays were performed using TaqMan Universal PCR Master mix (Applied Biosystems). The expression of the following genes was analyzed: *Cxcl1*, *Cxcl5*, *Il6*; data were normalized using the expression of the *Hprt1* gene (Applied Biosystems). *Nlrp2* expression was analyzed using the Sybr green probe (Roche); data were normalized using the expression of the *Gapdh* gene. Primer sequences are available on request. All data are expressed as arbitrary units (A.U.) using the 2^{-Dct} method [33].

2.5. Statistics

A preliminary power analysis showed that 6 mice per group were sufficient to assess normalization of CC16 urinary levels to normal values with an alpha error of 5 % and a power of 80 %, based on urinary CC16 excretion levels obtained in previous studies from our laboratory [34].

Data are expressed as mean ± SD or, if they are not normally distributed, as median and interquartile range [IQR]. Differences between groups were compared with ANOVA or with the Kruskal-Wallis test followed by pairwise comparisons with the uncorrected Dunn's test (if results were statistically significant after the Kruskal-Wallis test). All *p* values are two-sided and considered significant if <0.05. The GraphPad Prism software version 10 (GraphPad Software Inc., San Diego, CA, USA) was used for all statistical analyses.

3. Results

3.1. Luteolin did not affect growth, liver histology, and liver enzyme levels in Ctns $^{-/-}$ mice

Animals were fed with standard diet or with a luteolin supplemented diet (150 mg/kg/day) from 2 to 8 months of age. Somatic growth was unaffected by luteolin (Fig. 1A-B). To exclude hepatotoxicity after prolonged luteolin exposure, we evaluated liver histology and measured liver function tests after sacrifice. H&E staining sections showed normal liver histology in all animals, regardless of genotype and treatment group (Fig. 1C). Serum levels of liver enzymes at the age of 8 months showed no significant changes (Fig. 1D-F).

3.2. Luteolin reduced p62/SQSTM1 levels and lysosome defects in *Ctns*$^{-/-}$ mice

To evaluate the effects of luteolin on autophagy, we have quantified p62/SQSTM1 positive structures by immunofluorescence in cortical sections of kidneys harvested after sacrifice. As expected, p62/SQSTM1 mean intensity levels increased in renal tubular structures of knock out mice, compared to wild type mice (15.8 [11.6–19.6] vs. 8.4 [7.0–10.2], p <0.001; Fig. 2A). Luteolin treatment reduced significantly p62/SQSTM1 levels (11.7 [9.5–15.1], p <0.001; Fig. 2A), without however, restoring values to wild type levels.

Defects of the lysosomal compartment were also investigated (Fig. 2B). Lysosomal associated membrane protein 1 (LAMP1) immunostaining of kidney sections showed accumulation of high number of enlarged lysosomes in *Ctns*$^{-/-}$ mice compared to wild type mice (Fig. 2B). Results were analyzed by measuring the number of LAMP1-positive structures (111 [52−329] vs. 4.5 [1–9.5], p <0.001; Fig. 2C), the size of LAMP1-positive structures (7.1 [6.4–8.3] vs. 5.6 [4.4–7.5] squared pixels, p <0.001; Fig. 2D), and the total area, per microscopic field, occupied by LAMP1-positive structures (814 [328–2754] vs 31 [10-49] squared pixels, p <0.001; Fig. 2E). After luteolin treatment, all parameters improved in *Ctns*$^{-/-}$ mice: the percent of improvement was 54 % for the number of LAMP1-positive structures (51 [12−128], p = 0.02), 13 % for their size (6.2 [5.7–6.9], p = 0.007), and 61 % for the total area per microscopic field (319 [77−751], p = 0.01) (Fig. 2C-E). Although improved, the number of LAMP1-positive structures and the total area occupied by LAMP1-positive structures were not restored to wild type values.

3.3. Luteolin decreased apoptosis in the renal parenchyma of *Ctns*$^{-/-}$ mice

As expected, *Ctns*$^{-/-}$ mice displayed more apoptosis events (cleaved caspase-3 immunostaining) in their renal cortex compared to wild type mice (1.5 [1.0–2.6] vs. 0.9 [0.8–1.0], p <0.001) (Fig. 3A). Luteolin treatment significantly reduced kidney expression of cleaved caspase-3 in *Ctns*$^{-/-}$ mice (0.98 [0.78–1.14], p <0.001; Fig. 3A) to levels observed in wild type mice.

3.4. Luteolin did not prevent renal parenchymal inflammation

Infiltration of kidney parenchyma by CD68-positive cells (monocytes and macrophages) mediates at least in part, tissue damage of *Ctns*$^{-/-}$ animals. We have quantified the mean intensity of CD68 staining in renal parenchyma and observed a significant increase in samples obtained from *Ctns*$^{-/-}$ mice, compared to wild type mice (1.5 [1.2–2.9] vs 0.9 [0.8–1.0], p <0.001), which was not ameliorated by luteolin therapy (1.5 [1.1–2.3]) (Fig. 4A). To confirm these observations, we quantified by qPCR performed on total kidney homogenates the expression levels of specific pro-inflammatory mediators (Fig. 4B-E). The expression of *Nlrp2*, *Cxcl1*, and *Cxcl5* was increased in kidney sections obtained from *Ctns*$^{-/-}$ mice and did not decrease significantly after luteolin treatment. However, *Nlrp2* mRNA expression was no longer different when comparing wild type animals and knock out animals treated with luteolin. *Il6* expression was similar in all experimental groups.

3.5. Luteolin did not prevent the development of Fanconi syndrome and of kidney tissue damage

This mouse model of cystinosis shows evidence of proximal tubular dysfunction from the age of 4–6 months. Accordingly, we observed increased urinary excretion of CC16, glycosuria, and polyuria in *Ctns*$^{-/-}$ animals. These were not ameliorated by luteolin treatment. However, urine output was no longer different when comparing wild type animals and knock out animals treated with luteolin (Fig. 5A-C). Urinary albumin, calcium, and phosphate were measured at 8 months of age. We observed significant albuminuria and hypercalciuria in *Ctns*$^{-/-}$ mice regardless of luteolin treatment (Fig. 5D-F). Creatinine clearance at 8 months of age was comparable among all experimental groups (Fig. 5G). Serum levels of creatinine, urea, calcium and phosphate were measured at sacrifice (Table 1). Phosphate levels were mildly but significantly increased in *Ctns*$^{-/-}$ animals. No other differences were noted.

Kidneys harvested from treated and untreated *Ctns*$^{-/-}$ mice appeared equally pale (Fig. 6A). No significant changes were observed in kidney weight (Fig. 6B). Cystine content was increased in cystinotic kidneys and was not affected by luteolin therapy (Fig. 6C).

Semi-quantitative evaluation of kidney lesions was performed blindly on P.A.S. stained sections. The "tissue damage score" (see methods) showed only mild lesions that did not reach statistical significance, when paired comparisons were performed between experimental groups (Fig. 6D).

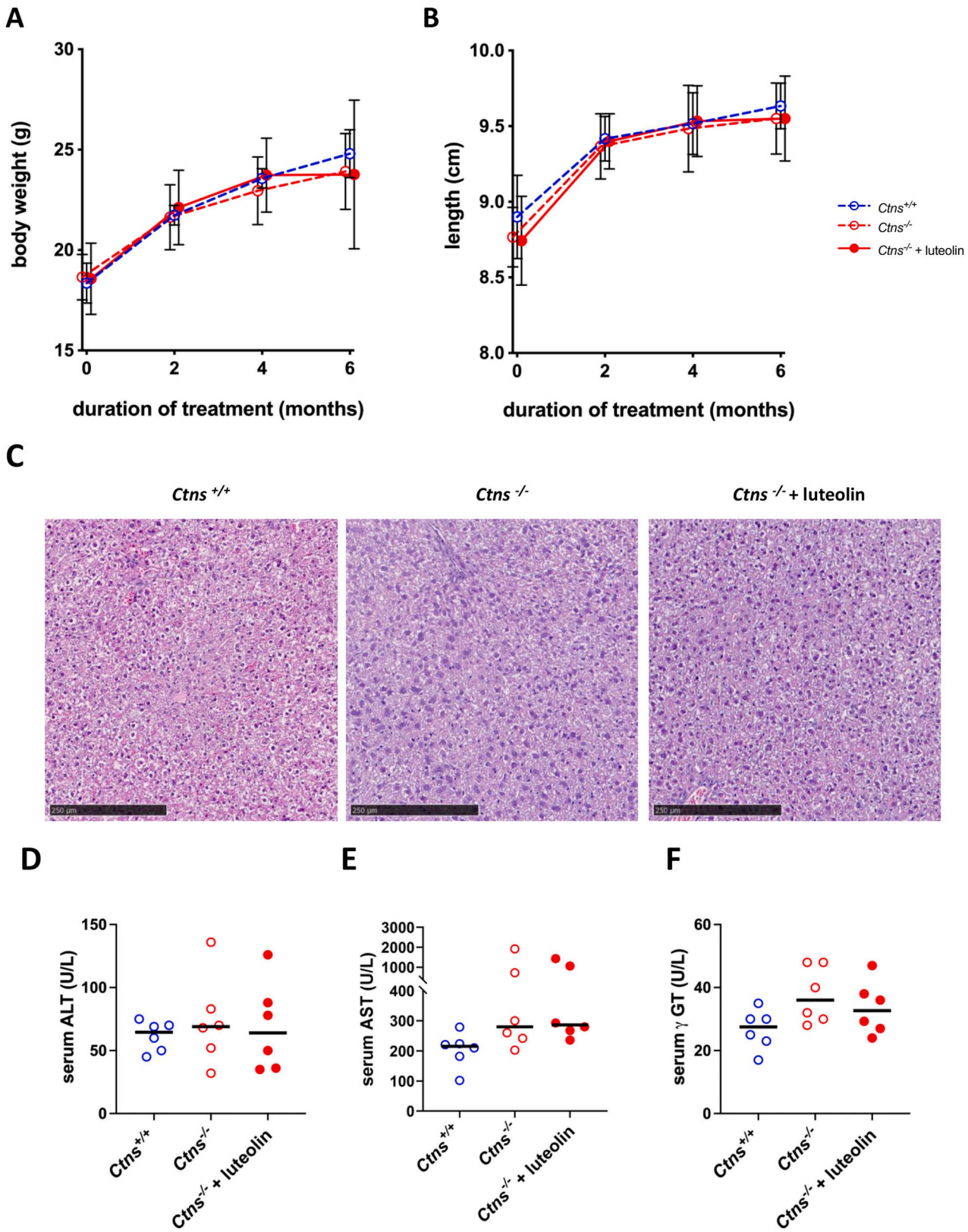

Fig. 1. Luteolin treatment did not affect growth and liver function. (A) Body weight and (B) body length were monitored starting from 2 months of age in *Ctns*$^{+/+}$, *Ctns*$^{-/-}$, and in *Ctns*$^{-/-}$ mice treated with luteolin for six months. Data are presented as mean ± SD (n = 6 mice for each experimental group). (C) Representative image of H&E-stained liver section from *Ctns*$^{+/+}$, *Ctns*$^{-/-}$ and *Ctns*$^{-/-}$ mice treated with luteolin. Scale bars: 250 µm. Serum level of (D) alanine aminotransferase (ALT), (E) aspartate aminotransferase (AST), and (F) gamma-glutamyl transferase (γGT). Each data point represents a single mouse (n = 6 mice for each experimental group); lines indicate median values. Differences between groups were compared using ANOVA or the Kruskal-Wallis tests. No significant differences were observed for all comparisons.

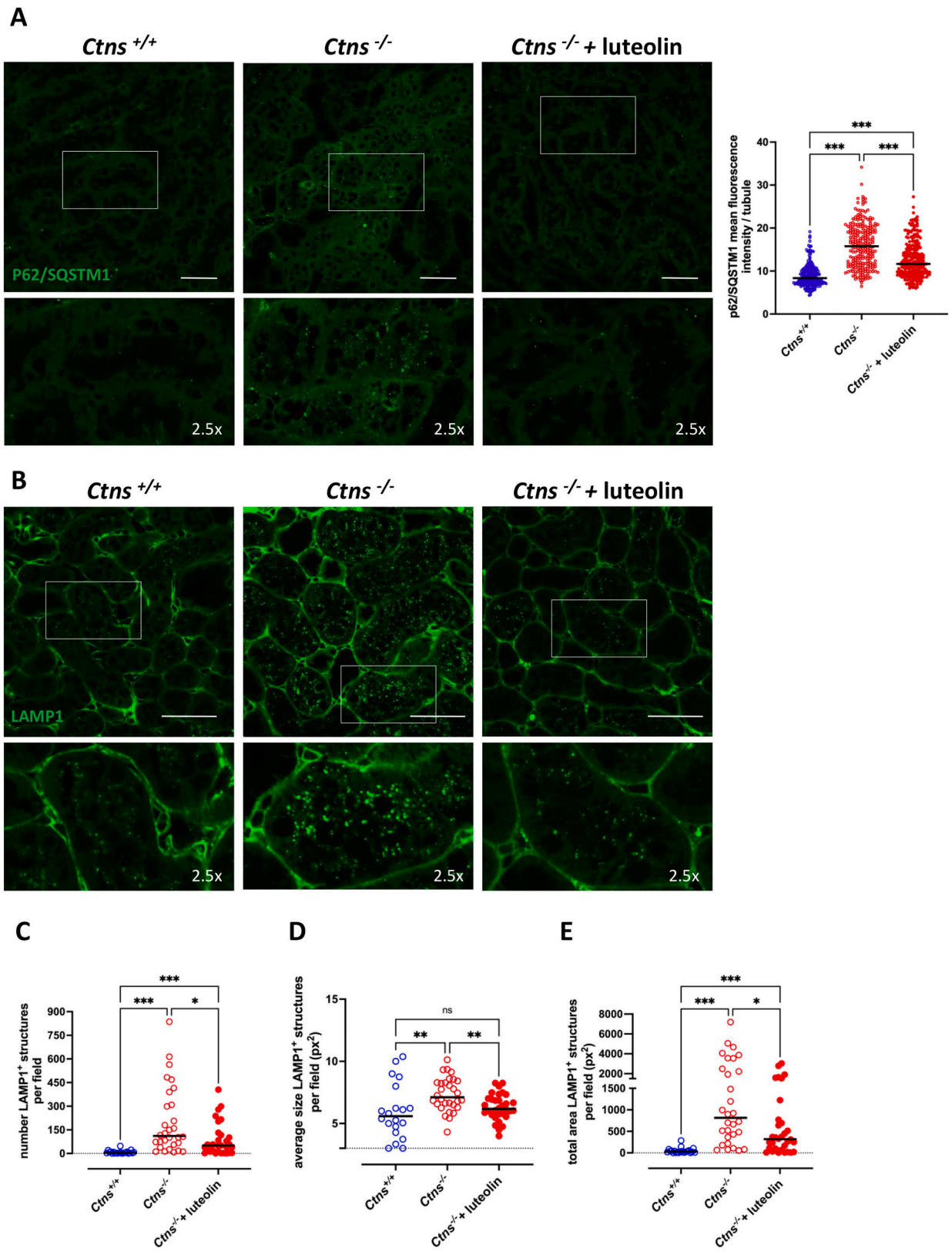

Fig. 2. Luteolin reduced p62/SQSTM1 levels and lysosome defects in *Ctns*$^{-/-}$ mice. (A) Representative confocal images and fluorescence quantification of p62/SQSTM1 expression in kidney sections from *Ctns*$^{+/+}$, *Ctns*$^{-/-}$ and *Ctns*$^{-/-}$ mice treated with luteolin. Scale bars: 20 μm. Lower panels, enlargements of the boxed areas. Each data point represents the mean fluorescence intensity in one tubular structure (n >200 tubules from 6 different mice per condition); lines indicate median values. (B) Representative confocal images of kidney section stained with LAMP1. Scale bars: 20 μm. Lower panels, enlargements of the boxed areas. (C-E) Quantification of LAMP1 positive structure in proximal tubules; each data point represents the number (C), average size (px^2) (D), and total area (px^2) (E), of LAMP1 positive structures in one field (n = 30 fields pooled from 6 mice per condition). Differences between groups were compared using the Kruskal-Wallis test and if significant, the uncorrected Dunn's test. Abbreviations: ns = non-significant; *p <0.05; **p <0.01; ***p <0.001.

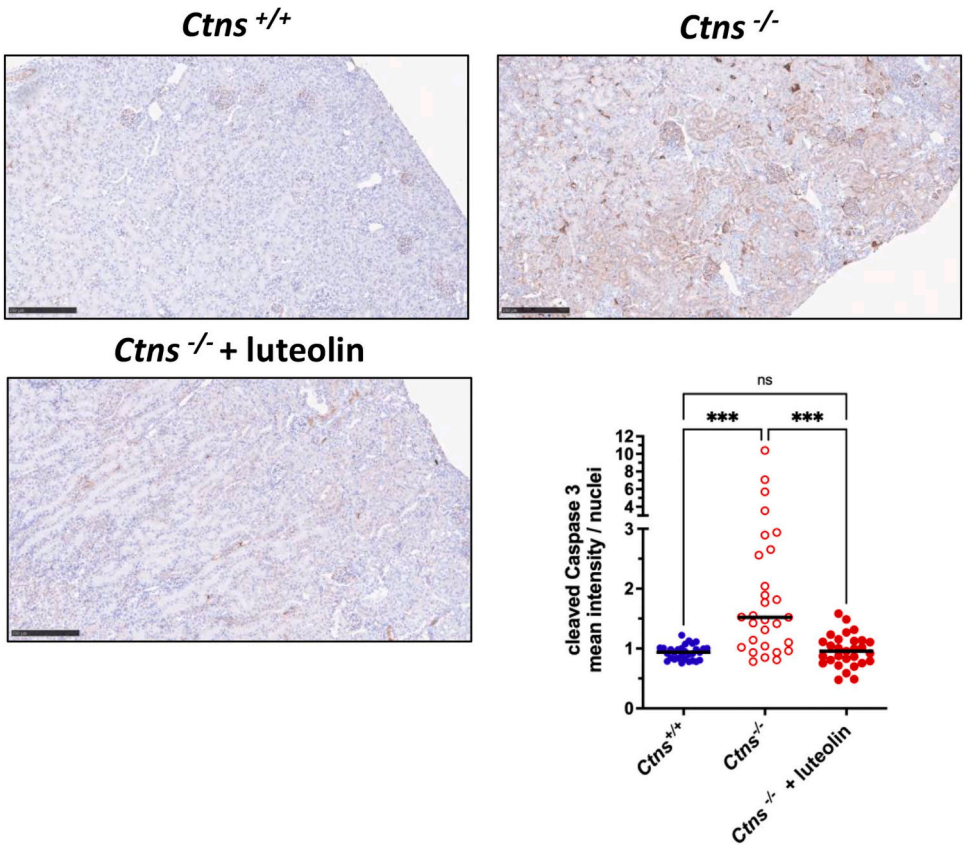

Fig. 3. Luteolin protected from apoptosis in *Ctns* $^{-/-}$ mice. (A) Representative image showing immunohistochemical staining for cleaved caspase 3 and quantification of cleaved caspase 3 in kidney cortex of *Ctns*$^{+/+}$, *Ctns*$^{-/-}$ and *Ctns*$^{-/-}$ mice treated with luteolin. Scale bars: 250 μm. Each data point represents the cleaved caspase 3 mean intensity normalized for the number of nuclei in one field (n = 30 fields pooled from 6 mice per condition). Differences between groups were compared using the Kruskal-Wallis test, and if significant, the uncorrected Dunn's test. Abbreviations: ns = non-significant; ***$p < 0.001$.

4. Discussion

Cysteamine is the current standard of care for cystinosis. It has improved dramatically the life expectancy of patients but cannot prevent completely the development of many complications and has side effects that limit patient compliance. In our previous work, we identified luteolin as a candidate drug for cystinosis [30]. In this work, we have used a mouse model of cystinosis and confirmed *in vivo* positive effects of luteolin on autophagy, lysosomal homeostasis, and apoptosis, but we did not observe a substantial protection against proximal tubular dysfunction.

Lysosomal engulfment in lysosomal storage diseases has been shown to produce several secondary changes in cells, including reduced endosomal trafficking, impaired autophagy, dysregulation of signaling pathways, abnormal calcium homeostasis, activation of inflammation, oxidative stress, and mitochondrial dysfunction [20,21,25,30,35,36]. In principle, by promoting cystine clearance from lysosomes, cysteamine should reverse these changes [20,21,25,30,36]. Recent studies have shown however, that some abnormal pathways, in particular autophagy, do not respond well to cysteamine despite normalization of cell cystine concentrations [21,30]. It has also been shown that cystinosin interacts with several cell proteins, including the mTORC1 complex, the vacuolar H^+ ATPase, and galectin 3, independently from its transport activity [37,38]. This has led to the hypothesis that incomplete response to cysteamine may be secondary to altered cellular pathways that are not related to lysosomal cystine accumulation. Targeting these pathways would therefore represent an attractive new therapeutic strategy.

Drug repositioning is particularly attractive in rare diseases [28,29]. We have previously used a high throughput in-cell ELISA screening assay to identify compounds that could rescue the accumulation of p62/SQSTM1 in cystinotic cells [30]. This study led to the identification of luteolin as a potential therapy for cystinosis. Luteolin is a natural flavonoid that is particularly rich in fruit and vegetables [39]. In secondary assays performed *in vitro* on cystinotic cells and *in vivo* using a zebrafish model of cystinosis, we have observed that luteolin can restore normal lysosomal distribution, improve megalin expression, ameliorate vesicular trafficking, and decrease the rate of apoptosis [30]. Preclinical studies in other diseases have also shown positive effects of luteolin on cell oxidation, tissue inflammation, unregulated growth, apoptosis, autophagy, aging, and neurodegeneration [31,39–42].

Luteolin was also particularly interesting because we have previously treated *Ctns*$^{-/-}$ mice with genistein, another flavonoid, and observed substantial protection of kidney parenchyma and kidney function [34,43]. After sacrifice, renal cystine content and cystine crystal accumulation were significantly decreased in animal treated with genistein, possibly because of increased lysosomal clearance by exocytosis [34,43]. Unlike luteolin however, genistein did not reduce *in vitro* the accumulation of p62/SQSTM1 (unpublished data). Luteolin could therefore provide additional activity on the autophagy defect of cystinosis. When administered to cystinotic cells and to zebrafish larvae, luteolin did not induce toxic effects, even at high concentrations [30]. Consistently, we did not observe significant side effects during a prolonged 6-month treatment in mice. This finding is in agreement with recent clinical trials, showing no major side effects of luteolin in humans [44,45]. We focused the toxicity evaluations on the liver because luteolin is concentrated and metabolized in hepatocytes [46].

As expected, our data showed that luteolin treatment decreased p62/SQSTM1 levels *in vivo*, improved abnormal lysosomal morphology, and decreased apoptosis in the renal cortex of treated animals. Unfortunately, it did not prevent the development of polyuria, of LMW

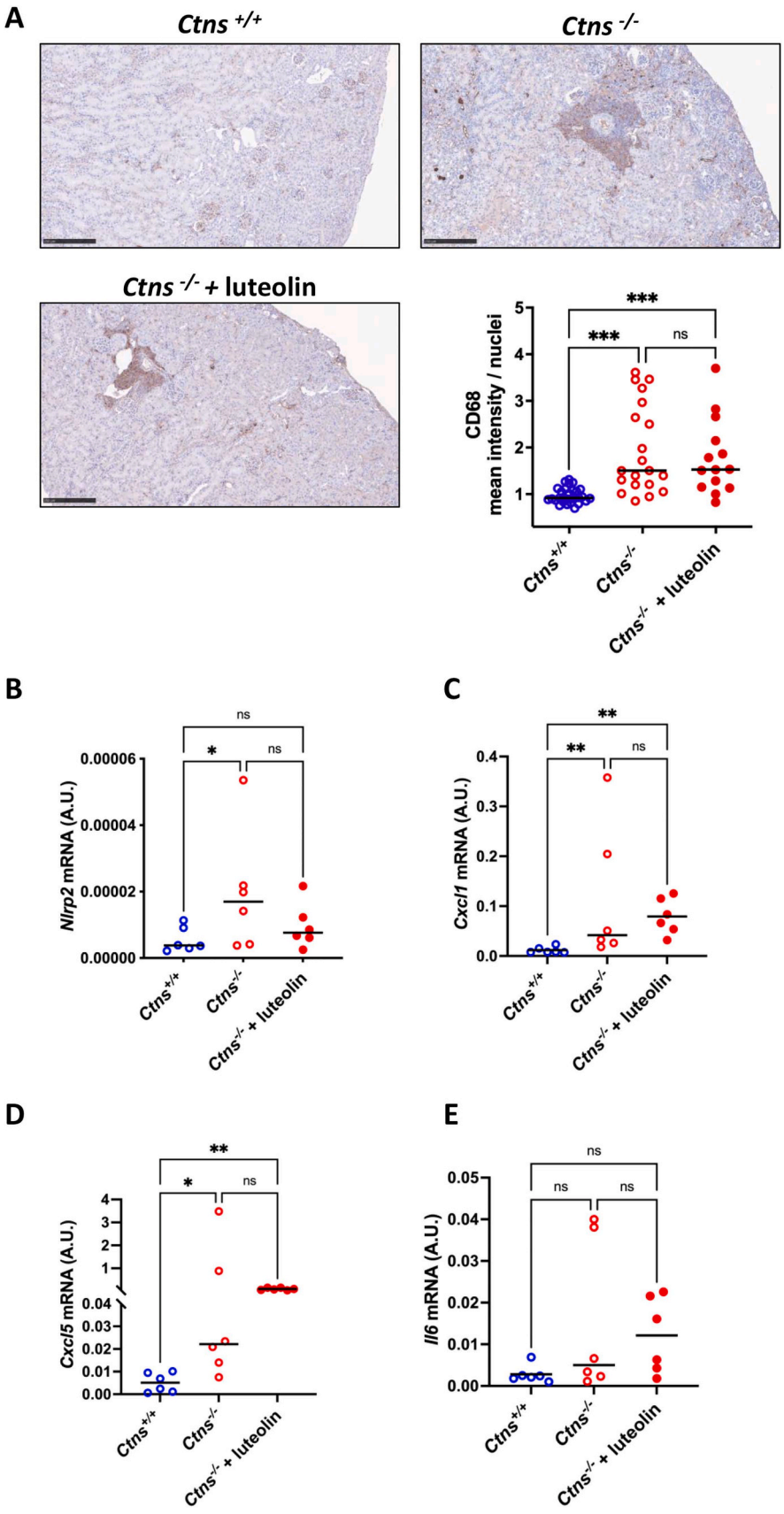

(caption on next page)

Fig. 4. Luteolin did not mitigate renal parenchymal inflammation. (A) Representative image of CD68 immunostaining and quantification in kidney cortex from *Ctns*$^{+/+}$, *Ctns*$^{-/-}$ and *Ctns*$^{-/-}$ mice treated with luteolin. Scale bars: 250 μm. Each data point represents CD68 immunostaining mean intensity normalized for the number of nuclei in one field (n = 30 fields pooled from 6 *Ctns*$^{+/+}$ or *Ctns*$^{-/-}$ mice and n = 15 fields pooled from 3 *Ctns*$^{-/-}$ mice treated with luteolin). (B) *Nlrp2*, (C) *Cxcl1*, (D) *Cxcl5* and (E) *Il6* mRNA expression levels evaluated by qPCR in total kidney homogenates; *Cxcl1*, *Cxcl5*, *Il6* data were normalized using the expression of the *Hprt1* gene. *Nlrp2* data were normalized using the expression of the *Gapdh* gene. All data are expressed as arbitrary units (n = 6 mice per condition). Differences between groups were compared using the nonparametric Kruskal-Wallis test, and if significant, the uncorrected Dunn's test. Abbreviations: A.U.: arbitrary units; ns = non-significant; *p <0.05; **p <0.01; ***p <0.001.

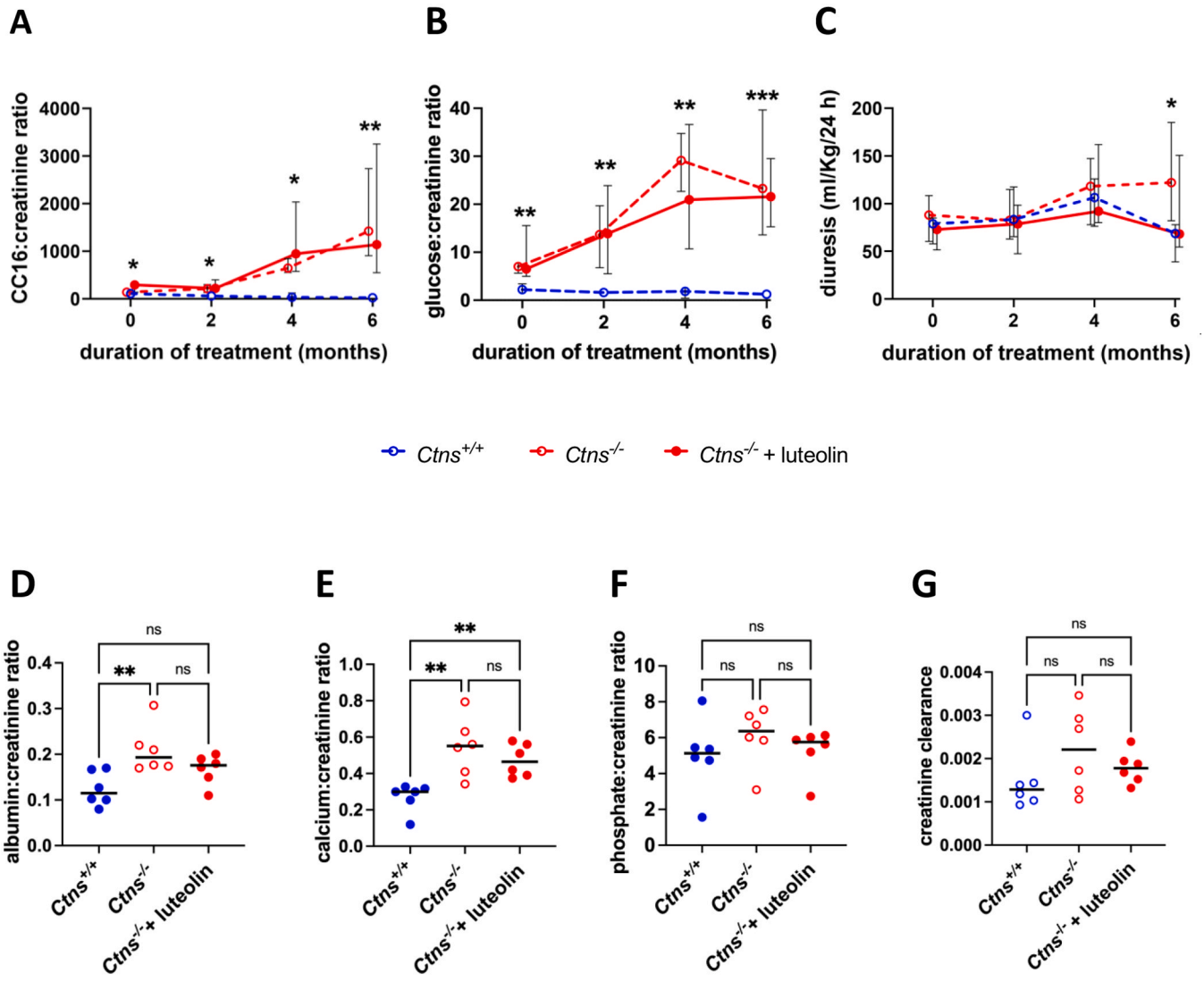

Fig. 5. Luteolin did not prevent development of proximal tubular dysfunction. (A-G) Urinary parameters of Fanconi syndrome and kidney function: (A) urinary LMW proteins (CC16)/creatinine ratio, (B) glucose/creatinine ratio, (C) 24 h diuresis normalized for body weight, (D) albumin/creatinine ratio, (E) calcium/creatinine ratio, (F) phosphate/creatinine ratio, and (G) creatinine clearance. The latter 4 parameters were calculated only at sacrifice in 8-month old mice. (A-C): data are expressed as median values and interquartile range (n = 6); (D-G) each data-point represent a single animal; line indicate median values. Differences between groups in each timepoint were compared using the nonparametric Kruskal-Wallis test, and if significant, the uncorrected Dunn's test. Statistically significant differences in (A-C) are presented for wild-type versus *Ctns*$^{-/-}$ mice, only. Abbreviations: ns = non-significant; *p <0.05; **p <0.01; ***p <0.001.

proteinuria, and of glycosuria, which are the main signs of renal Fanconi syndrome in Ctns$^{-/-}$ mice [22,24,32]. Contrary to genistein [34,43], luteolin did not reduce cystine accumulation in kidneys.

Lack of efficacy of luteolin on tubular disease was somewhat unexpected. In zebrafish, we previously observed that luteolin preserved significantly megalin expression [30]. Moreover, it has been shown that primary tubular cells derived from *Ctns*$^{-/-}$ mice are exposed to increased oxidative stresses as a consequence of altered autophagy, which decreases the clearance of damaged mitochondria that release radical species in the cytosol [20]. By improving autophagic processes, we were expecting that luteolin would protect proximal tubular cells.

We cannot exclude that higher dose of luteolin, which has a relatively low bioavailability [47], would have been more efficient. However, the discrepancy between the observed improvements in lysosomal distribution, autophagy, and cell apoptosis in the renal cortex and the lack of effects of luteolin on renal Fanconi syndrome is remarkable.

Alternatively, our results may be explained by the ineffectiveness of luteolin in reducing cystine accumulation and renal parenchyma inflammation.

In respect to cystine accumulation, it was unanimously believed until

Table 1
Serum parameters at sacrifice (8-month-old mice).

	Ctns$^{+/+}$ untreated (n=6)	*Ctns*$^{-/-}$ untreated (n=6)	*Ctns*$^{-/-}$ luteolin (n=6)
Creatinine (mg/dL)	1.03 [0.99–1.00]	0.84 [0.61–1.14]	0.80 [0.64–1.00]
Urea (mg/dL)	54.50 [52.25–58.00]	41.50 [21.50–56.75]	33.00 [25.00–45.00]
Calcium (mg/dL)	8.06 [7.70–8.43]	8.03 [7.9–8.53]	7.93 [7.46–8.37]
Phosphate (mg/dL)	10.45 [10.25–10.65]	11.24 [10.79–13.28] **	10.80 [9.81–11.67]

Data are presented as median values and interquartile range [p25-p75]. Comparisons where made between *Ctns*$^{-/-}$ mice and untreated wild type animals using the nonparametric Kruskal-Wallis test followed by the uncorrected Dunn's test, if significant. Unless specified, differences did not reach statistical significance. Abbreviations: ** $p < 0.01$.

recently, that cysteamine has no effects on renal Fanconi syndrome in humans and therefore, that lysosomal cystine accumulation is not the cause of proximal tubular dysfunction in cystinosis. At odds with this view, studies performed in *Ctns*$^{-/-}$ mice have shown that cystine crystals play a pivotal role in promoting tubular cell damage and that early cysteamine therapy can prevent tubular dysfunction [24,34]. To reconcile these observations, lack of efficacy of cysteamine in humans may be explained by the timing of initiation of treatment, which is nearly always started late, when Fanconi syndrome has already developed. A recent retrospective analysis of six patients that were diagnosed early by family screening has shown that cysteamine can in fact mitigate proximal tubular dysfunction also in humans [48].

In respect to inflammation, previous data have shown that inflammation plays a significant role in the progression of tissue damage in cystinosis. The Nod-like receptor protein 2 (NLRP2) for example, is markedly upregulated in cystinotic human PTCs [49] and invalidation of the *Nlrp2* gene in *Ctns*$^{-/-}$ mice has been shown to delay the development of chronic kidney lesions [50]. Also, galectin-3 is a proinflammatory protein that interacts with cystinosin and promotes inflammation in its free cytosolic form [38]. Invalidation of the *Gal-3* gene in *Ctns*$^{-/-}$ mice ameliorates kidney function, delays the development of renal fibrosis, and reduces renal inflammatory cell infiltration [38]. Further supporting the role of inflammation in tissue damage of cystinosis, treatment of *Ctns*$^{-/-}$ mice with the IL-1β inhibitor anakinra can reverse fat browning and muscle wasting [51]. In our experiments, inflammatory cell infiltration, transcription of *Nlrp2*, and transcription of inflammatory cytokines/chemokines were not reduced after luteolin treatment. This was particularly surprising, since we had previously observed a significant reduction (>60 %) in *NLRP2* and *IL6 mRNA* expression after treating immortalized cystinotic human PTCs with luteolin at a concentration of 50 μM for up to 24 h (unpublished data).

This study has some limitations. Kidneys were harvested at 8 months of age. At that age, parenchymal kidney lesions are variable and not very pronounced in this mouse model, while kidney function is usually still preserved and polyuria is modest [22,24,32,34,52]. This prevented detecting possible beneficial effects of luteolin on the development of polyuria and chronic kidney lesions. Lack of effects on kidney inflammation suggests however, that luteolin is probably not efficient in preventing chronic kidney failure, in this mouse model. In addition, mice do not mimic completely the human phenotype: compared to humans, they develop proportionally later tubular dysfunction and chronic kidney failure, they do not develop proximal tubular acidosis, and have only mild or no phosphaturia [53].

5. Conclusions

Results of the present study have confirmed the effects of luteolin on several cellular pathways that are impaired in cystinosis, confirming our previous data *in vitro*. However, these results failed to translate into significant pre-clinical benefits. The search for additional treatment for cystinosis is ongoing. In addition to hematopoietic stem cell

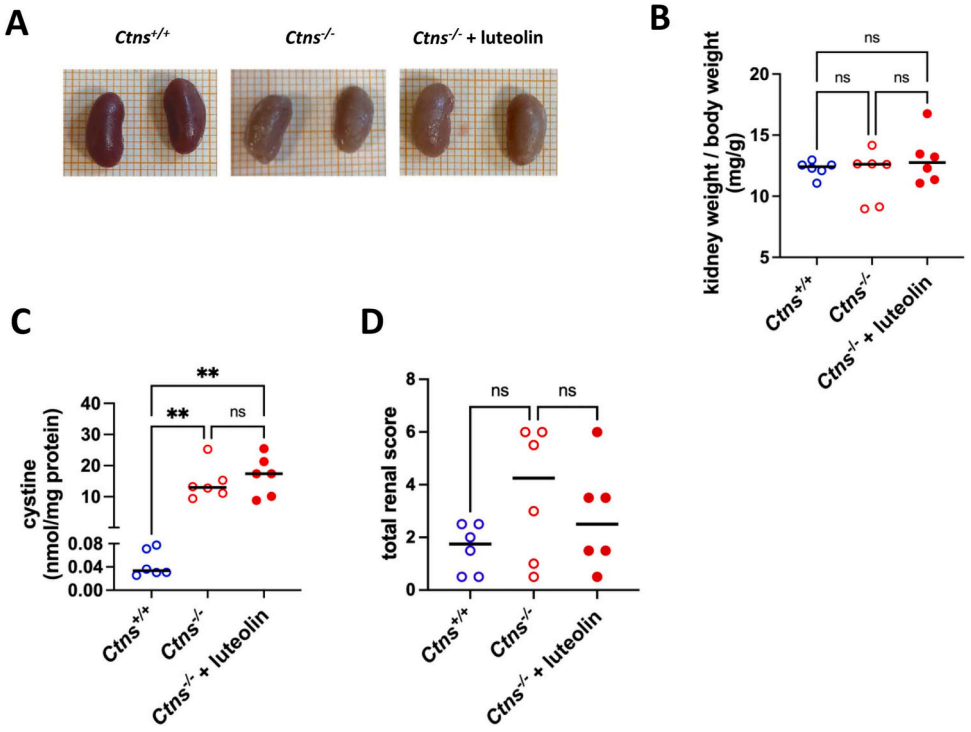

Fig. 6. Morphological and histological kidney analysis. (A) Representative images of kidneys harvested from 8 months-old *Ctns*$^{+/+}$, *Ctns*$^{-/-}$ and *Ctns*$^{-/-}$ mice treated with luteolin. (B) Kidney weight normalized for body weight (n = 6). (C) Cystine levels in total kidney lysate normalized for protein content (n = 6). (D) Tissue damage score (see methods for details). Each data-point represent a single animal, line indicate median values. Differences between groups were compared using the nonparametric Kruskal-Wallis test, and if significant, the uncorrected Dunn's test. Abbreviations: ns = non-significant; **$p < 0.01$.

transplantation after *ex-vivo* gene therapy [9], other molecules acting directly or indirectly on autophagy have been proposed and are being tested, including mTOR inhibitors [54,55] and stimulators of chaperon mediated autophagy [56,57].

Funding

This work was supported by the Cystinosis Research Foundation (grant number #CRF-2016–004) to F. E. and L.R.R. and Italian Ministry of Health, (5x1000 2022) to E. D. L..

CRediT authorship contribution statement

Francesco Bellomo: Writing – review & editing, Validation, Formal analysis, Data curation. **Michela Piccione:** Investigation. **Marco Pezzullo:** Investigation. **Alessia Vitale:** Methodology, Investigation. **Valentina Matteo:** Validation, Investigation, Formal analysis. **Laura Rita Rega:** Writing – review & editing, Visualization, Supervision, Funding acquisition, Data curation. **Ester De Leo:** Writing – review & editing, Writing – original draft, Visualization, Supervision, Investigation, Formal analysis, Data curation, Conceptualization. **Giusi Prencipe:** Writing – review & editing, Validation, Formal analysis. **Roberto Raso:** Validation, Investigation, Data curation. **Francesco Emma:** Writing – review & editing, Writing – original draft, Visualization, Supervision, Funding acquisition, Conceptualization. **Anna Taranta:** Writing – review & editing, Investigation, Formal analysis, Data curation. **Francesca Diomedi Camassei:** Validation, Investigation, Formal analysis. **Bianca Maria Goffredo:** Methodology.

Declaration of Competing Interest

The authors declare no conflict of interest.

Acknowledgements

The authors thank Dr. Cristiano De Stefanis for technical contribution and Dr. Manuela Colucci for supervising statistical analysis. The authors also thank Cystinosis Research Foundation (grant number #CRFF-2020-003) for supporting G.P and Italian Ministry of Health with Current Research funds and Fondazione Bambino Gesù ("Vite Coraggiose 2 – Una diagnosi per la Cura," progetto CC-2018-2366307) for supporting M.P.

References

[1] V. Kalatzis, S. Cherqui, C. Antignac, B. Gasnier, Cystinosin, the protein defective in cystinosis, is a H+-driven lysosomal cystine transporter, EMBO J. 20 (2001) 5940–5949, https://doi.org/10.1093/emboj/20.21.5940.

[2] M.J. Wilmer, F. Emma, E.N. Levtchenko, The pathogenesis of cystinosis: mechanisms beyond cystine accumulation, Am. J. Physiol. Ren. Physiol. 299 (2010), https://doi.org/10.1152/ajprenal.00318.2010.

[3] F. Emma, W. van t. Hoff, K. Hohenfellner, R. Topaloglu, M. Greco, G. Ariceta, C. Bettini, D. Bockenhauer, K. Veys, L. Pape, S. Hulton, S. Collin, F. Ozaltin, A. Servais, G. Deschênes, R. Novo, A. Bertholet-Thomas, J. Oh, E. Cornelissen, M. Janssen, D. Haffner, L. Ravà, C. Antignac, O. Devuyst, P. Niaudet, E. Levtchenko, An international cohort study spanning five decades assessed outcomes of nephropathic cystinosis, Kidney Int (2021), https://doi.org/10.1016/j.kint.2021.06.019.

[4] W.A. Gahl, J.G. Thoene, J.A. Schneider, Medical progress: cystinosis, N. Engl. J. Med. 347 (2002) 111–121, https://doi.org/10.1056/NEJMra020552.

[5] J.G. Thoene, R.G. Oshima, J.C. Crawhall, Intracellular cystine depletion by aminothiols in vitro and in vivo, J. Clin. Investig. 58 (1976), https://doi.org/10.1172/JCI108448.

[6] W.A. Gahl, G.F. Reed, J.G. Thoene, J.D. Schulman, W.B. Rizzo, A.J. Jonas, D. W. Denman, J.J. Schlesselman, B.J. Corden, J.A. Schneider, Cysteamine therapy for children with nephropathic cystinosis, N. Engl. J. Med 316 (1987) 971–977, https://doi.org/10.1056/NEJM198704163161602.

[7] A. Brodin-Sartorius, M.J. Tête, P. Niaudet, C. Antignac, G. Guest, C. Ottolenghi, M. Charbit, D. Moyse, C. Legendre, P. Lesavre, P. Cochat, A. Servais, Cysteamine therapy delays the progression of nephropathic cystinosis in late adolescents and adults, Kidney Int 81 (2012), https://doi.org/10.1038/ki.2011.277.

[8] W.A. Gahl, J.Z. Balog, R. Kleta, Nephropathic cystinosis in adults: natural history and effects of oral cysteamine therapy, Ann. Intern Med 147 (2007), https://doi.org/10.7326/0003-4819-147-4-200708210-00006.

[9] A. Jamalpoor, A. Othman, E.N. Levtchenko, R. Masereeuw, M.J. Janssen, Molecular mechanisms and treatment options of nephropathic cystinosis, Trends Mol. Med 27 (2021) 673–686, https://doi.org/10.1016/j.molmed.2021.04.004.

[10] M. Park, A. Helip-Wooley, J. Thoene, Lysosomal cystine storage augments apoptosis in cultured human fibroblasts and renal tubular epithelial cells, J. Am. Soc. Nephrol. 13 (2002), https://doi.org/10.1097/01.ASN.0000036867.49866.59.

[11] M.A. Park, V. Pejovic, K.G. Kerisit, S. Junius, J.G. Thoene, Increased apoptosis in cystinotic fibroblasts and renal proximal tubule epithelial cells results from cysteinylation of protein kinase Cδ, J. Am. Soc. Nephrol. 17 (2006) https://doi.org/10.1681/ASN.2006050474.

[12] J.G. Thoene, Lysosomal cystine augments apoptosis and causes the phenotype in cystinosis, Beijing Da Xue Xue Bao. Yi Xue Ban. = J. Peking. Univ. Health Sci. 37 (2005).

[13] A. Taranta, F. Bellomo, S. Petrini, E. Polishchuk, E. De Leo, L.R. Rega, A. Pastore, R. Polishchuk, M.A. De Matteis, F. Emma, Cystinosin-LKG rescues cystine accumulation and decreases apoptosis rate in cystinotic proximal tubular epithelial cells, Pedia Res 81 (2017) 113–119, https://doi.org/10.1038/pr.2016.184.

[14] D. De Rasmo, A. Signorile, E. De Leo, E.V. Polishchuk, A. Ferretta, R. Raso, S. Russo, R. Polishchuk, F. Emma, F. Bellomo, Mitochondrial dynamics of proximal tubular epithelial cells in nephropathic cystinosis, Int J. Mol. Sci. 21 (2020), https://doi.org/10.3390/ijms21010192.

[15] F. Bellomo, A. Signorile, G. Tamma, M. Ranieri, F. Emma, D. De Rasmo, Impact of atypical mitochondrial cyclic-AMP level in nephropathic cystinosis, Cell. Mol. Life Sci. 75 (2018) 3411–3422, https://doi.org/10.1007/s00018-018-2800-5.

[16] M.J.G. Wilmer, A. De Graaf-Hess, H.J. Blom, H.B.P.M. Dijkman, L.A. Monnens, L. P. Van Den Heuvel, E.N. Levtchenko, Elevated oxidized glutathione in cystinotic proximal tubular epithelial cells, Biochem Biophys. Res Commun. 337 (2005), https://doi.org/10.1016/j.bbrc.2005.09.094.

[17] M.H. Vaisbich, L. Pache de Faria Guimaraes, M.H.M. Shimizu, A.C. Seguro, Oxidative stress in cystinosis patients, Nephron Extra 1 (2011), https://doi.org/10.1159/000331445.

[18] R. Sumayao, B. McEvoy, P. Newsholme, T. McMorrow, Lysosomal cystine accumulation promotes mitochondrial depolarization and induction of redox-sensitive genes in human kidney proximal tubular cells, J. Physiol. 594 (2016) 3353–3370, https://doi.org/10.1113/JP271858.

[19] G. Prencipe, I. Caiello, S. Cherqui, T. Whisenant, S. Petrini, F. Emma, F. De Benedetti, Inflammasome activation by cystine crystals: implications for the pathogenesis of cystinosis, J. Am. Soc. Nephrol. 25 (2014), https://doi.org/10.1681/ASN.2013060653.

[20] B.P. Festa, Z. Chen, M. Berquez, H. Debaix, N. Tokonami, J.A. Prange, G. van de Hoek, C. Alessio, A. Raimondi, N. Nevo, R.H. Giles, O. Devuyst, A. Luciani, Impaired autophagy bridges lysosomal storage disease and epithelial dysfunction in the kidney, Nat. Commun. 9 (2018) 161, https://doi.org/10.1038/s41467-017-02536-7.

[21] G. Napolitano, J.L. Johnson, J. He, C.J. Rocca, J. Monfregola, K. Pestonjamasp, S. Cherqui, S.D. Catz, Impairment of chaperone-mediated autophagy leads to selective lysosomal degradation defects in the lysosomal storage disease cystinosis, EMBO Mol. Med 7 (2015) 158–174, https://doi.org/10.15252/emmm.201404223.

[22] C. Raggi, A. Luciani, N. Nevo, C. Antignac, S. Terryn, O. Devuyst, Dedifferentiation and aberrations of the endolysosomal compartment characterize the early stage of nephropathic cystinosis, Hum. Mol. Genet 23 (2014) 2266–2278, https://doi.org/10.1093/hmg/ddt617.

[23] E.A. Ivanova, M.G. De Leo, L. Van Den Heuvel, A. Pastore, H. Dijkman, M.A. De Matteis, E.N. Levtchenko, Endo-lysosomal dysfunction in human proximal tubular epithelial cells deficient for lysosomal cystine transporter cystinosin, PLoS One 10 (2015) e0120998, https://doi.org/10.1371/journal.pone.0120998.

[24] H.P. Gaide Chevronnay, V. Janssens, P. Van Der Smissen, F. N'Kuli, N. Nevo, Y. Guiot, E. Levtchenko, E. Marbaix, C.E. Pierreux, S. Cherqui, C. Antignac, P. J. Courtoy, Time course of pathogenic and adaptation mechanisms in cystinotic mouse kidneys, J. Am. Soc. Nephrol. 25 (2014), https://doi.org/10.1681/ASN.2013060598.

[25] P. Krohn, L.R. Rega, M. Harvent, B.P. Festa, A. Taranta, A. Luciani, J. Dewulf, A. Cremonesi, F.D. Camassei, J.V.M. Hanson, C. Gerth-Kahlert, F. Emma, M. Berquez, O. Devuyst, Multisystem involvement, defective lysosomes and impaired autophagy in a novel rat model of nephropathic cystinosis, Hum. Mol. Genet 31 (2022) 2262–2278, https://doi.org/10.1093/hmg/ddac033.

[26] S. Cherqui, P.J. Courtoy, The renal Fanconi syndrome in cystinosis: pathogenic insights and therapeutic perspectives, Nat. Rev. Nephrol. 13 (2017), https://doi.org/10.1038/nrneph.2016.182.

[27] L.R. Rega, E. De Leo, D. Nieri, A. Luciani, Defective cystinosin, aberrant autophagy−endolysosome pathways, and storage disease: towards assembling the puzzle, Cells 11 (2022), https://doi.org/10.3390/cells11030326.

[28] F. Bellomo, E. De Leo, A. Taranta, L. Giaquinto, G. Di Giovamberardino, S. Montefusco, L.R. Rega, A. Pastore, D.L. Medina, D. Di Bernardo, M.A. De Matteis, F. Emma, Drug repurposing in rare diseases: an integrative study of drug screening and transcriptomic analysis in nephropathic cystinosis, Int J. Mol. Sci. 22 (2021), https://doi.org/10.3390/ijms222312829.

[29] A. Taranta, M.A. Elmonem, F. Bellomo, E. De Leo, S. Boenzi, M.J. Janssen, A. Jamalpoor, S. Cairoli, A. Pastore, C. De Stefanis, M. Colucci, L.R. Rega, I. Giovannoni, P. Francalanci, L.P. van den Heuvel, C. Dionisi-Vici, B.M. Goffredo, R. Masereeuw, E. Levtchenko, F. Emma, Benefits and toxicity of disulfiram in preclinical models of nephropathic cystinosis, Cells 10 (2021), https://doi.org/10.3390/cells10123294.

[30] E. De Leo, M.A. Elmonem, S.P. Berlingerio, M. Berquez, B.P. Festa, R. Raso, F. Bellomo, T. Starborg, M.J. Janssen, Z. Abbaszadeh, S. Cairoli, B.M. Goffredo, R. Masereeuw, O. Devuyst, M. Lowe, E. Levtchenko, A. Luciani, F. Emma, L. R. Rega, Cell-based phenotypic drug screening identifies luteolin as candidate therapeutic for nephropathic cystinosis, J. Am. Soc. Nephrol. 31 (2020), https://doi.org/10.1681/ASN.2019090956.

[31] S.F. Nabavi, N. Braidy, O. Gortzi, E. Sobarzo-Sanchez, M. Daglia, K. Skalicka-Woźniak, S.M. Nabavi, Luteolin as an anti-inflammatory and neuroprotective agent: a brief review, Brain Res Bull. 119 (2015), https://doi.org/10.1016/j.brainresbull.2015.09.002.

[32] N. Nevo, M. Chol, A. Bailleux, V. Kalatzis, L. Morisset, O. Devuyst, M.-C. Gubler, C. Antignac, Renal phenotype of the cystinosis mouse model is dependent upon genetic background, Nephrol. Dial. Transpl. 25 (2010) 1059–1066, https://doi.org/10.1093/ndt/gfp553.

[33] R. Harshitha, D.R. Arunraj, Real-time quantitative PCR: a tool for absolute and relative quantification, Biochem. Mol. Biol. Educ. 49 (2021), https://doi.org/10.1002/bmb.21552.

[34] E. De Leo, A. Taranta, R. Raso, E. Polishchuk, V. D'Oria, M. Pezzullo, B. M. Goffredo, S. Cairoli, F. Bellomo, G. Battafarano, F.D. Camassei, A. Del Fattore, R. Polishchuk, F. Emma, L.R. Rega, Genistein improves renal disease in a mouse model of nephropathic cystinosis: a comparison study with cysteamine, Hum. Mol. Genet 32 (2023) 1090–1101, https://doi.org/10.1093/hmg/ddac266.

[35] G. Parenti, D.L. Medina, A. Ballabio, The rapidly evolving view of lysosomal storage diseases, EMBO Mol. Med 13 (2021), https://doi.org/10.15252/emmm.202012836.

[36] A. Luciani, B.P. Festa, Z. Chen, O. Devuyst, Defective autophagy degradation and abnormal tight junction-associated signaling drive epithelial dysfunction in cystinosis, Autophagy 14 (2018) 1157–1159, https://doi.org/10.1080/15548627.2018.1446625.

[37] Z. Andrzejewska, N. Nevo, L. Thomas, C. Chhuon, A. Bailleux, V. Chauvet, P. J. Courtoy, M. Chol, I. Chiara Guerrera, C. Antignac, Cystinosin is a component of the vacuolar H+-ATPase-ragulator-rag complex controlling mammalian target of rapamycin complex 1 signaling, J. Am. Soc. Nephrol. 27 (2016), https://doi.org/10.1681/ASN.2014090937.

[38] T. Lobry, R. Miller, N. Nevo, C.J. Rocca, J. Zhang, S.D. Catz, F. Moore, L. Thomas, D. Pouly, A. Bailleux, I.C. Guerrera, M.C. Gubler, W.W. Cheung, R.H. Mak, T. Montier, C. Antignac, S. Cherqui, Interaction between galectin-3 and cystinosin uncovers a pathogenic role of inflammation in kidney involvement of cystinosis, Kidney Int 96 (2019), https://doi.org/10.1016/j.kint.2019.01.029.

[39] M. Lopez-Lazaro, Distribution and biological activities of the flavonoid luteolin, Mini-Rev. Med. Chem. 9 (2008), https://doi.org/10.2174/138955709787001712.

[40] N. Muruganathan, A.R. Dhanapal, V. Baskar, P. Muthuramalingam, D. Selvaraj, H. Aara, M.Z.S. Abdullah, I. Sivanesan, Recent updates on source, biosynthesis, and therapeutic potential of natural flavonoid luteolin: a review, Metabolites 12 (2022), https://doi.org/10.3390/metabo12111145.

[41] M. Ashrafizadeh, Z. Ahmadi, T. Farkhondeh, S. Samarghandian, Autophagy regulation using luteolin: new insight into its anti-tumor activity, Cancer Cell Int 20 (2020), https://doi.org/10.1186/s12935-020-01634-9.

[42] F. Gendrisch, P.R. Esser, C.M. Schempp, U. Wölfle, Luteolin as a modulator of skin aging and inflammation, BioFactors 47 (2021), https://doi.org/10.1002/biof.1699.

[43] L.R. Rega, E. Polishchuk, S. Montefusco, G. Napolitano, G. Tozzi, J. Zhang, F. Bellomo, A. Taranta, A. Pastore, R. Polishchuk, F. Piemonte, D.L. Medina, S. D. Catz, A. Ballabio, F. Emma, Activation of the transcription factor EB rescues lysosomal abnormalities in cystinotic kidney cells, Kidney Int 89 (2016) 862–873, https://doi.org/10.1016/j.kint.2015.12.045.

[44] S. Terzo, A. Amato, A. Magán-Fernández, G. Castellino, P. Calvi, R. Chianetta, R. V. Giglio, A.M. Patti, D. Nikolic, A. Firenze, F. Mulè, M. Ciaccio, M. Rizzo, A nutraceutical containing chlorogenic acid and luteolin improves cardiometabolic parameters in subjects with pre-obesity: a 6-month randomized, double-blind, placebo-controlled study, Nutrients 15 (2023), https://doi.org/10.3390/nu15020462.

[45] A. Taliou, E. Zintzaras, L. Lykouras, K. Francis, An open-label pilot study of a formulation containing the anti-inflammatory flavonoid luteolin and its effects on behavior in children with autism spectrum disorders, Clin. Ther. 35 (2013), https://doi.org/10.1016/j.clinthera.2013.04.006.

[46] G. Du, L. Fu, J. Jia, X. Pang, H. Yu, Y. Zhang, G. Fan, X. Gao, L. Han, Validated UPLC-MS/MS method for quantification of seven compounds in rat plasma and tissues: application to pharmacokinetic and tissue distribution studies in rats after oral administration of extract of Eclipta prostrata L, Biomed. Chromatogr. 32 (2018), https://doi.org/10.1002/bmc.4191.

[47] D. Yuan, Y. Guo, F. Pu, C. Yang, X. Xiao, H. Du, J. He, S. Lu, Opportunities and challenges in enhancing the bioavailability and bioactivity of dietary flavonoids: a novel delivery system perspective, Food Chem. 430 (2024), https://doi.org/10.1016/j.foodchem.2023.137115.

[48] K. Hohenfellner, C. Nießl, D. Haffner, J. Oh, C. Okorn, K. Palm, K.P. Schlingmann, S. Wygoda, W.A. Gahl, Beneficial effects of starting oral cysteamine treatment in the first 2 months of life on glomerular and tubular kidney function in infantile nephropathic cystinosis, Mol. Genet Metab. 136 (2022), https://doi.org/10.1016/j.ymgme.2022.06.009.

[49] M.N. Rossi, A. Pascarella, V. Licursi, I. Caiello, A. Taranta, L.R. Rega, E. Levtchenko, F. Emma, F. De Benedetti, G. Prencipe, NLRP2 regulates proinflammatory and antiapoptotic responses in proximal tubular epithelial cells, Front Cell Dev. Biol. 7 (2019), https://doi.org/10.3389/fcell.2019.00252.

[50] M.N. Rossi, V. Matteo, F. Diomedi-Camassei, E. De Leo, O. Devuyst, M. Lamkanfi, I. Caiello, E. Loricchio, F. Bellomo, A. Taranta, F. Emma, F. De Benedetti, G. Prencipe, Nlrp2 deletion ameliorates kidney damage in a mouse model of cystinosis, Front Immunol. (2024), https://doi.org/10.3389/fimmu.2024.1373224.

[51] W.W. Cheung, S. Hao, R. Zheng, Z. Wang, A. Gonzalez, P. Zhou, H.M. Hoffman, R. H. Mak, Targeting interleukin-1 for reversing fat browning and muscle wasting in infantile nephropathic cystinosis, J. Cachex-.-. Sarcopenia Muscle 12 (2021), https://doi.org/10.1002/jcsm.12744.

[52] W.W. Cheung, S. Cherqui, W. Ding, M. Esparza, P. Zhou, J. Shao, R.L. Lieber, R. H. Mak, Muscle wasting and adipose tissue browning in infantile nephropathic cystinosis, J. Cachex-.-. Sarcopenia Muscle 7 (2016), https://doi.org/10.1002/jcsm.12056.

[53] C.I. Galarreta, M.S. Forbes, B.A. Thornhill, C. Antignac, M.C. Gubler, N. Nevo, M. P. Murphy, R.L. Chevalier, The swan-neck lesion: proximal tubular adaptation to oxidative stress in nephropathic cystinosis, Am. J. Physiol. Ren. Physiol. 308 (2015), https://doi.org/10.1152/ajprenal.00591.2014.

[54] J.A. Hollywood, A. Przepiorski, R.F. D'Souza, S. Sreebhavan, E.J. Wolvetang, P. T. Harrison, A.J. Davidson, T.M. Holm, Use of human induced pluripotent stem cells and kidney organoids to develop a cysteamine/mtor inhibition combination therapy for cystinosis, J. Am. Soc. Nephrol. 31 (2020), https://doi.org/10.1681/ASN.2019070712.

[55] M. Berquez, Z. Chen, B.P. Festa, P. Krohn, S.A. Keller, S. Parolo, M. Korzinkin, A. Gaponova, E. Laczko, E. Domenici, O. Devuyst, A. Luciani, Lysosomal cystine export regulates mTORC1 signaling to guide kidney epithelial cell fate specialization, Nat. Commun. 14 (2023), https://doi.org/10.1038/s41467-023-39261-3.

[56] J. Zhang, J.L. Johnson, J. He, G. Napolitano, M. Ramadass, C. Rocca, W.B. Kiosses, C. Bucci, Q. Xin, E. Gavathiotis, A.M. Cuervo, S. Cherqui, S.D. Catz, Cystinosin, the small GTPase Rab11, and the Rab7 effector RILP regulate intracellular trafficking of the chaperone-mediated autophagy receptor LAMP2A, J. Biol. Chem. 292 (2017), https://doi.org/10.1074/jbc.M116.764076.

[57] J. Zhang, J. He, J.L. Johnson, F. Rahman, E. Gavathiotis, A.M. Cuervo, S.D. Catz, Chaperone-mediated autophagy upregulation rescues megalin expression and localization in cystinotic proximal tubule cells, Front Endocrinol. (Lausanne) 10 (2019), https://doi.org/10.3389/fendo.2019.00021.